A Comparative Study on One-month Solar Radiation Datasets for Photovoltaic Energy Analysis in Trondheim

Mattia Manni[1], Alessandro Nocente[2], Kristian Stenerud Skeie[2], Martin Bellmann[2] and Gabriele Lobaccaro[1]

[1] Department of Civil and Environmental Engineering, Norwegian University of Science and Technology (NTNU), Trondheim (Norway)

[2] SINTEF AS, Trondheim (Norway)

Abstract

This study presents a comparative study on one-month solar radiation datasets for solar energy analysis in Trondheim. Such datasets differ among the sources (i.e., satellite observations, reanalysis, weather stations), the radiative parameters (i.e., global horizontal irradiance, diffuse horizontal irradiance, and direct normal irradiance), and the time resolutions (i.e., one-minute, one-hour). The plane of array irradiance amounts impinging on a photovoltaic panel are determined through the decomposition and transposition models implemented in the pvlib-python tool or measured with a pyranometer oriented as the photovoltaic panels. Then, the photovoltaic energy production is quantified and validated against experimental data and the accuracy of the estimation is evaluated with the Mean Biased Error (MBE) and the Root Mean Squared Error (RMSE). Data about photovoltaic energy generation are collected from the Zero Emission Building (ZEB) Test Cell Laboratory, in Trondheim (Norway). The main research goal is to determine which dataset can better estimate photovoltaic energy production in the chosen location. Datasets providing direct measures of the plane of array irradiance or direct normal and diffuse horizontal irradiance amounts allow to reduce the length of the model chain. In particular, the dataset with the hourly plane of array irradiance observations from the ZEB Test Cell Laboratory permits quantifying the hourly energy generation from photovoltaics with the highest accuracy (MBE is 3.97 Wh, RMSE is 45.60 Wh). The results demonstrated how the datasets based on observations are more accurate than the datasets based on satellite imaging or numerical reanalysis.

Keywords: Photovoltaic, Solar energy, Simulations, Monitoring, High latitudes.

1. Introduction

In the era of the energy transition towards a low-carbon society, it is necessary, among the others, to boost the exploitation of renewable energy sources (RES), to improve the energy efficiency of building stock towards energy positive districts, and to promote sustainable development actions (e.g., decarbonisation, greenification). In that regard, the deployment of RES and high energy efficiency measures can potentially contribute to 90% of the required greenhouse gas emissions (GHG) reductions (International Renewable Energy Agency, 2022).

The solar and wind energy represent the main drivers of the low-carbon energy transition. In particular, the solar photovoltaic (PV) showed the highest growth rate (average annual increase of 36% in the past 30 years) among the RES (International Energy Agency, 2021a). PV is expected to account for 13% of the power production by 2030 compared with the current 1.7% (International Renewable Energy Agency, 2022), and to cover up to 33% of the total global energy needs by 2050 (International Energy Agency, 2021b).

Within this framework, new opportunities for solar energy production are actively investigated in Norway to counterbalance the growing energy demand which is currently satisfied by hydropower and wind power. In Norway, the solar energy showed the greatest growth throughout the last five years and the installed solar power has increased from 3 MW (2015) to 140 MW (2020) (Fig. 1) (Energy Facts Norway, 2021). The misconception that the level of irradiation is much lower in the Nordics than in the Continental Europe partially contributed to such a delay in the exploitation of solar energy (Formolli et al., 2021). However, there are some advantages in installing PV systems at high latitudes like the high efficiency due to the low temperatures and the significant

doi:10.18086/eurosun.2022.15.03 Available at http://proceedings.ises.org

amount of solar energy which is reflected by the snow covering the ground (Dubey et al., 2013).

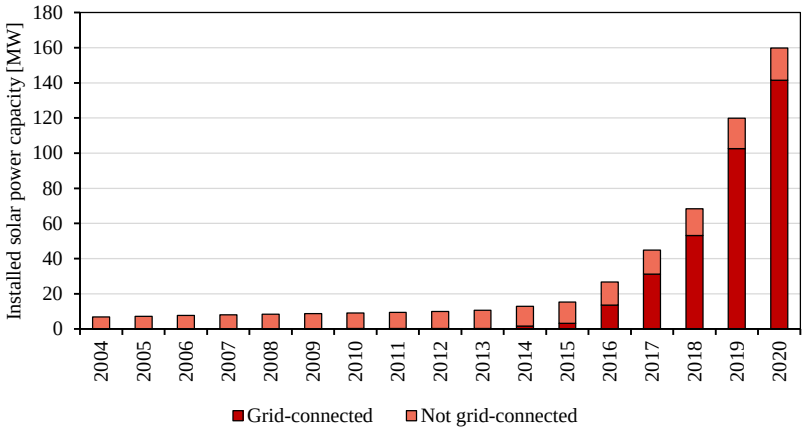

Fig 1: Development in installed capacity for solar power in Norway (Energy Facts Norway, 2021).

To boost more the solar energy penetration in Norway, it is necessary to design highly effective PV and to implement a model chain to accurately simulate their energy generation. Although the high number of overcast days (particularly in the wintertime) makes difficult to estimate the global irradiation impinging on PV, recent advancements in solar irradiance model chain enables more precise calculations methods (Yang, 2022). Decomposition models exploiting one-minute radiation datasets have been implemented to evaluate instantaneous effects such as the cloud and albedo enhancement, while some hourly transposition models appear to be equally applicable to one-minute data (Gueymard, 2017).

The present study focuses on the investigation of the influence of different solar radiation datasets on PV energy simulation. One-month solar radiation datasets for Trondheim location are retrieved from various sources (i.e., satellite observations, weather station) and then used as input parameters in the pvlib-python package (Holmgren et al., 2018) to estimate the plane of array irradiance (POA). The comparative analysis of the results against experimental data permits to preliminary identify the most adequate datasets to be used in PV energy analysis. In this context, this study is part of a wider research which aims at developing a model chain for prediction of energy generation from PV to be applied to high latitudes.

The paper is structured as follows: the section of materials and methods (section 2) defines the workflow, the exploited datasets, the tools, the accuracy indicators, and the case study; the section of results and discussion (section 3) provides an overview of the outcomes, discuss the PV analysis capability of the datasets, and outlines the study limitations. The study concludes with a summary of the most relevant findings and the implications for future advancements in model chain development and application at high latitudes (section 4).

2. Materials and methods

2.1. Workflow

The workflow is structured in four steps: (i) decomposition modelling, (ii) transposition modelling, (iii) PV energy assessment, and (iv) experimental validation (Fig. 2). In the first step, the global horizontal irradiation (GHI) is input to quantify the diffuse horizontal irradiation (DHI) and the direct normal irradiation (DNI) as outputs. The DNI and the DHI are considered as inputs in the second step. In the second step, the DHI and DNI are transposed from the horizontal plane to a tilted surface, and the POA is calculated. The tilted surface is defined according to the geometry properties of the PV panel (i.e., tilt angle, azimuth angle). Then, the amounts of POA are used to estimate PV energy generation. Finally, the modelled PV energy generation is validated against experimental data from the Zero Emission Building (ZEB) Test Cell Laboratory located at the Norwegian University of Science and Technology (NTNU) Gløshaugen Campus in Trondheim, Norway (Latitude 63.4305° N).

The model chain described in the workflow is flexible and its length (i.e., the number of steps) can change depending on the input. For example, if a dataset providing the DNI and DHI values is selected, the step about decomposition modelling is skipped, and the model chain is shortened. Thus, the full-length model chain starts

from step one and it includes decomposition, transposition, and energy modelling, while the shortest possible model chain has POA as input and it starts from step three.

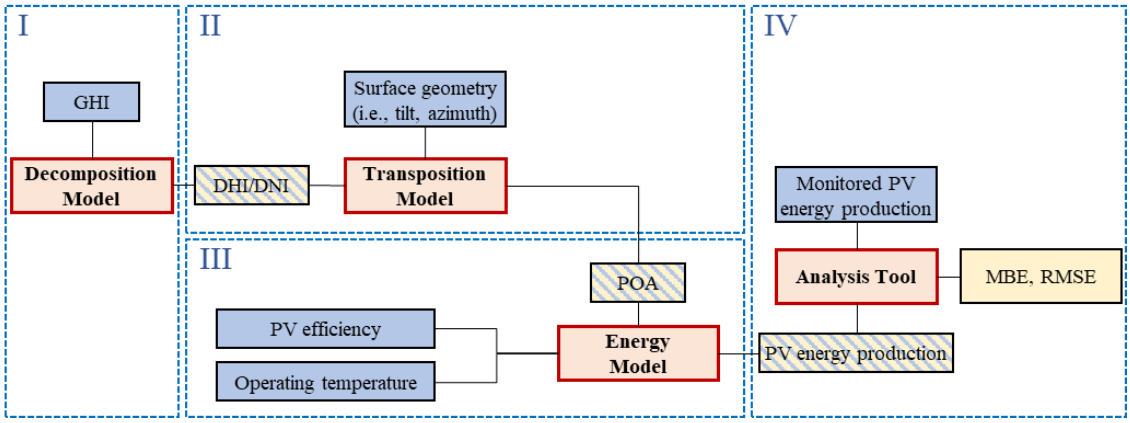

Fig. 2: Overview of the workflow followed in this study. The workflow is structured in four steps: (i) decomposition modelling, (ii) transposition modelling, (iii) PV energy assessment, and (iv) experimental validation.

2.2. Datasets

Weather datasets used in this work refer to Trondheim. The climate of Trondheim is classified as continental subartic climate (Dfc) in Köppen Geiger classification (Fig. 3) and it is moderately continental, with cold winters and mild summers. The analyses are carried out for the month of October 2021. The selected one-month datasets are characterized by a time resolution ranging from one minute to one hour depending on the source.

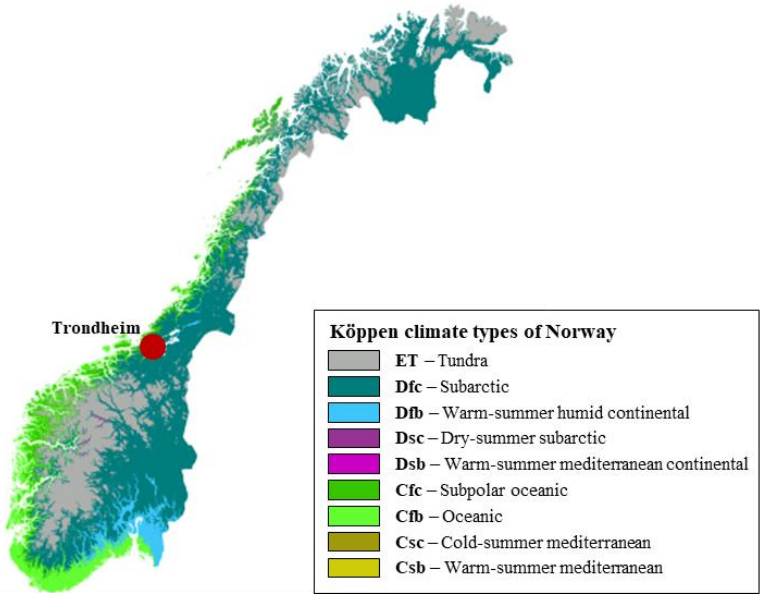

Fig. 3: The Köppen climate classification. Modified from "Köppen climate types of Norway" by Adam Peterson.

An overview of the used datasets and their principal properties (i.e., data type, time resolution, spatial resolution, parameters) is presented in Tab. 1. The month of October has been selected to assess the viability of the datasets to estimate the PV generation outputs during days characterized by overcast sky conditions. Before calculating the accuracy indicators (see sub-section 2.4), the datasets are resampled hourly, daily, and monthly.

Among the datasets provided by the European Centre for Medium-Range Weather Forecasts (ECMWF), the 5th generation of numerical reanalysis (ERA5-Land) is selected. ERA5-Land consists of a version of ERA5 which is specifically developed for land applications. According to the different field of applications, the spatial resolution of ERA5-Land (9 km) is greater than the one of ERA5 (around 30 km). Data cover a time horizon ranging from January 1950 to present, and concern the main variables related to temperature, lakes, snow, soil water, radiation and heat, evaporation, wind, pressure, and precipitation. The variables retrieved from the Copernicus Climate

Data Store for the time domain of this work (October 2021) are the surface solar radiation downwards (corresponding to the global horizontal irradiation), both the temperature and the dewpoint temperature at two meters from the ground, and the surface pressure. In particular, the accumulated radiation values of ERA5-Land are transformed to hourly values by subtracting the previous values within each forecast horizon.

Tab. 1: Characteristics of the datasets used in this study.

Data source	Data type	Timestep	Spatial resolution	Parameters
ERA5-land	Reanalysis	1 hour	9 km	GHI
CAMS	Satellite data	1 minute	3-5 km	DHI, DNI, GHI
Sentralbygg	Monitored data	1 minute	point	DHI, DNI, GHI
Test Cell Lab	Monitored data	5 minutes	point	GHI
Test Cell Lab	Monitored data	1 hour	point	GTI
Test Cell Lab	Monitored data	1 hour	point	PV energy generation

The Copernicus Atmosphere Monitoring Service (CAMS) Solar Radiation service combines output from the CAMS global forecast system on aerosol and ozone with detailed cloud information directly from geostationary satellites. The CAMS Solar Radiation service provides, among the others, historical values (2004 to present) of GHI, DHI, and DNI (both overcast and clear sky conditions) with a time resolution of 1 minute. Such irradiance parameters were retrieved for October 2021.

Alongside reanalysis and satellite observation, the amounts of solar irradiance are also measured through sensors installed in various facilities at the NTNU Gløshaugen campus. In particular, the hourly values of GHI and POA are collected through two pyranometers installed on the rooftop of the Test Cell Lab, while the DHI and the DNI are measured through a sun tracker located at the top of the tower of the Sentralbygg. The sun tracker follows the sun path over the horizon to orient the pyrheliometer in the same direction of the sunrays as well as to keep in the shadow the pyranometer which measures the DHI. The system is completed by an unshaded pyranometer which monitors the GHI. Different time resolutions are associated to these datasets, ranging from 1 minute (DNI and DHI) to 1 hour (POA). The GHI values are recorded every 5 minutes.

Finally, the energy generation from the PV panels installed on the rooftop of the Test Cell Lab is monitored with a time resolution of 1 hour. This timeseries is compared to the simulated ones which result from the different solar irradiance datasets.

2.3. Tools

The PV energy generation output is calculated using the pvlib-python package, an open-source and community-supported tool that simulates the performance of PV systems. The tool allows managing the whole model chain from the irradiance decomposition to the transposition process, and to the PV energy simulation. In particular, pvlib-python includes methods like the Perez model that are well established for hourly irradiance decomposition methods, and some one-minute decomposition methods (Yang, 2022). These models differ for the accuracy and for the predictors which are needed to estimate the diffuse fraction. In this study, the Engerer4 model is exploited to decompose the GHI into DNI and DHI. The model has been implemented by Bright and Engerer (Bright and Engerer, 2019) who updated the Engerer2 model by recalculating the parameters with datasets from 75 different stations worldwide.

Regarding the transposition models, the Perez anisotropic model is used since is the one exploited almost universally in building performance simulation, although other options are available in the pvlib-python package (e.g., the isotropic model (Loutzenhiser et al., 2007), the Hay-Davies model (Hay, 1993), and the Reindl model (Reindl et al., 1990)). The Perez model splits the diffuse irradiance into different components (i.e., isotropic, circumsolar, horizontal brightening band) and then estimate the amount of irradiance achieving the PV modules. The solar position (i.e., solar azimuth, solar zenith, apparent solar time) is one of the Perez model's input parameters, and it is estimated with the ephemeris function from the pvlib-python package.

Finally, the POA is used to estimate the energy amount generated by the PV panels. The energy generated by PV

modules is calculated with a simple equation from the EN 15316- 4-3:2017 standard:

$$E_{el,out} = \frac{E_{sol,pv} \cdot P_{pk} \cdot f_{perf}}{I_{ref}}$$

where $E_{sol,pv}$ is the solar irradiation impinging on the system expressed in Wh/m^2, P_{pk} is the system peak power in kW at reference conditions (I_{ref}= 1 kW/m^2).

The system performance factor, f_{perf}, accounts for losses due to soiling (φ_{soil}) and temperature (φ_{temp}), as well as to the specific array's configuration (φ_{array}) and the inverter's efficiency (η_{inv}). It is calculated according to the Norwegian technical guideline SN-NSPEK 3031:

$$f_{perf} = IAM \cdot \left(1 - \frac{\varphi_{soil}}{100}\right) \cdot \left(1 - \frac{\varphi_{temp}}{100}\right) \cdot \left(1 - \frac{\varphi_{array}}{100}\right) \cdot \frac{\eta_{inv}}{100}$$

where IAM is the Incident Angle Modifier. The η_{inv} equals 96%, while the IAM, is defined based on the empirical values proposed in the standard for the Trondheim location and the selected months. In particular, the IAM is 0.96, the φ_{soil} ranges between 2% and 5%, and the φ_{array} is 5.5%. Finally, the φ_{temp} depends on the cell's temperature (T_{cell}), and it is estimated as:

$$\varphi_{temp} = \alpha_{temp} \cdot (T_{cell} - 25°C)$$

where α_{temp} is a temperature coefficient and equals 0.40% per Celsius degree.

2.4. Accuracy indicators for PV output timeseries and data quality filter

To compare the capability of the different solar radiation datasets to estimate PV energy generation with overcast sky conditions, the Mean Bias Error (MBE) and the Root Mean Square Error (RMSE) are used. The two coefficients are defined as it follows:

$$MBE = \frac{1}{N} \cdot \sum_{i=1}^{N} (\bar{x}_i - x_i)$$

$$RMSE = \sqrt{\frac{1}{N} \cdot \sum_{i=1}^{N} (\bar{x}_i - x_i)^2}$$

where the $\bar{x}_i$ and the x_i are the simulated and the measured photovoltaic energy generation amounts, respectively.

A data quality filter (DQF) is applied to the measurements by excluding periods where the solar elevation is lower than 5 degrees. In fact, when solar elevation is lower than 5 degrees, the incidence angle of the solar beams on the sensor is very high, and thus, it can result in less accurate measurements. Evaluation metrics are calculated before and after the DQF is applied.

2.5. Case study

The ZEB Test Cell Laboratory (Fig. 4) consists of a large- and full-scale test cell building facility used, among the others, for outdoor natural climate testing of building materials, components, building management strategies and structure elements. This research facility is equipped with three different PV panels which are integrated in the rooftop. The three PV panels are made, respectively, of monocrystalline, polycrystalline, and amorphous solar cells and their energy production is monitored with a one-hour time resolution. Data from the polycristalline silicon (poly-Si) modules are used in the experimental validation of the model chain implemented in this study. The polycrystalline silicon modules are the 260PE series from REC. Each module is 1.65 m^2 and has 60 cells and 3 bypass diodes. The rated power is 260 W_p per module and the rated efficiency is 15.8%. Four modules, with a total power of 1040 W_p, are installed on the roof with a tilt and an azimuth angles of 40° abd 180°, respectively. The three solar panels are connected to a micro-converter/inverter system from SolarEdge enabling each module to always operate at the best possible conditions. The benefit of the micro-converter system is to prevent the whole string output to be reduced if a single module is shaded.

Fig. 4: Test Cell Lab facility at NTNU Gløshaugen campus. Pictures from: www.sintef.no.

3. Results and discussion

3.1. PV simulation over different time resolutions

Outcomes from the model chain described in section 2 are reported in the scatter plots in the Fig. 5 and Fig. 6. In particular, the observed PV outputs are showed against the modelled PV outputs which derives from:

- POA measured in the Test Cell Lab (gti_tc),
- DNI and DHI monitored in the Sentralbygg (dni/dhi_sb),
- GHI recorded in the Test Cell Lab (ghi_tc),
- DNI and DHI retrieved from CAMS (dni/dhi_cams),
- GHI calculated by ERA5-Land (ghi_era).

It is worth to highlight that the whole dataset is considered in the graphs in Fig. 5, while only the values satisfying the DQF requirements are considered in the graphs in Fig. 6. Hence, the length of the datasets is reduced from 300 to 224 datapoints.

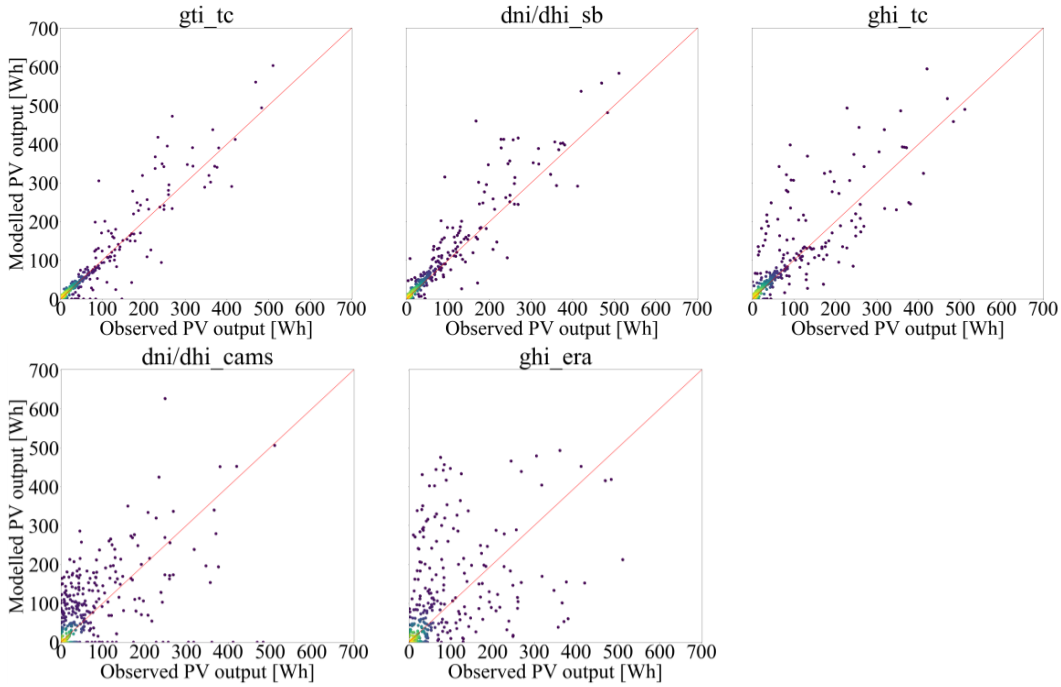

Fig. 5: Hourly observed PV energy production and modelled PV energy production during October 2021, before data quality filter. The yellow color indicates a high datapoint density, while the blue color represents a low datapoint density.

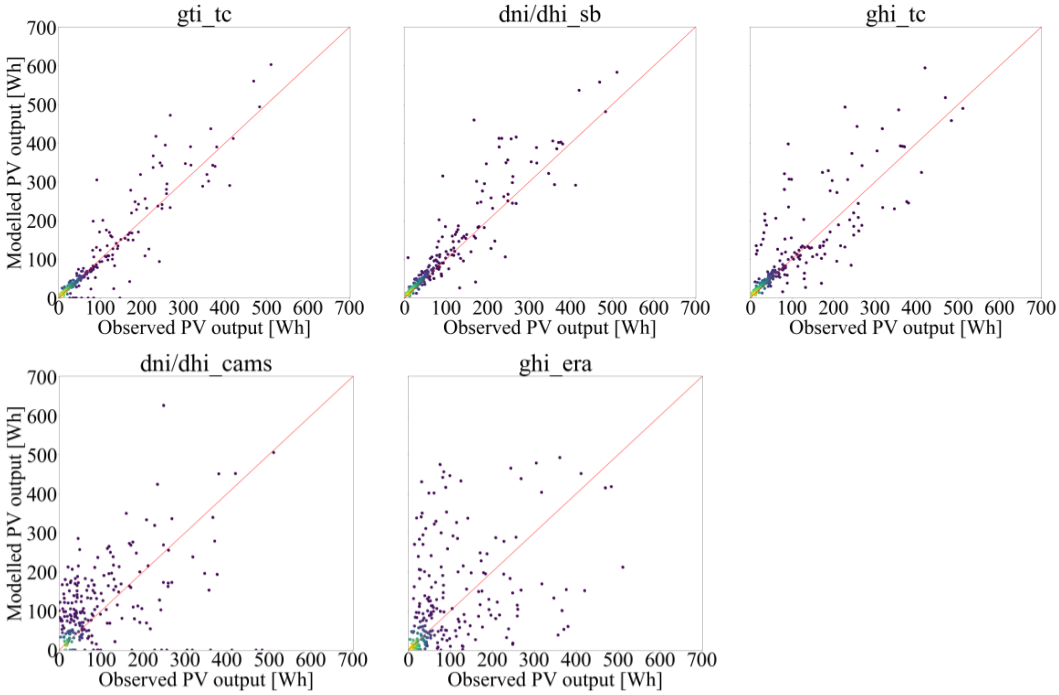

Fig. 6: Hourly observed PV energy production and modelled PV energy production during October 2021, after data quality filter. The yellow color indicates a high datapoint density, while the blue color represents a low datapoint density.

The plot of the results enables some preliminary considerations. Firstly, the monitored POA, DHI, and DNI values can estimate the energy generated by PV better than the others. Secondly, datasets from satellite observations are good as the datasets from Era5-Land reanalysis in PV simulation.

The accuracy indicators calculated for the five datasets confirmed such observations (Tab. 2). Before the DQF is applied, the model chain exploiting data of POA from the Test Cell Lab shows an MBE of 1.70 Wh and a RMSE of 25.50 Wh. These are the accuracy indicators corresponding to the best performance, while the worst results are obtained when satellite observations (MBE is 15.97 Wh, RMSE is 55.09 Wh) and numerical reanalysis are used (MBE is 11.95 Wh, RMSE is 83.50 Wh).

Tab. 2: Accuracy indicators calculated for the hourly datasets exploited in this study.

	gti_tc	**dni/dhi_sb**	**ghi_tc**	**dni/dhi_cams**	**ghi_era**
MBE [Wh]	1.70	5.70	6.26	15.97	11.95
RMSE [Wh]	25.50	28.96	42.10	55.09	83.50
MBE (DQF) [Wh]	3.97	16.61	12.87	37.48	23.71
RMSE (DQF) [Wh]	45.60	51.02	67.34	91.21	139.28

The application of the DQF leads to a general worsening of the PV simulation capability of the datasets. Although with a different magnitude, all the indicators are increased. In particular, the MBE calculated for the gti_tc is increased up to 3.97 Wh, while the RMSE is 45.60 Wh. The highest drop in the estimation performance is observed for dni/dhi_cams whose accuracy indicators are more than doubled (MBE is 37.48 Wh, RMSE is 91.21 Wh). Alongside these, the DNI and DHI values measured in the Sentralbygg (MBE is 16.61 Wh, RMSE is 51.02 Wh) calculated the PV energy generation better than the GHI values monitored in the Test Cell Lab (MBE is 12.87 Wh, RMSE is 67.34 Wh).

When it comes to the daily PV energy generation, the comparison between the measured values and the model outputs are reported in Fig. 7 and Fig. 8. It is worth to highlight that in this case the DQF causes the reduction of the observed amounts (i.e., amount of energy generated by the PV panel) and not the number of observations (i.e.,

number of recorded elements). As observed in the plots depicting the hourly values (see Fig. 5 and Fig. 6), the measured quantities better approximate the PV energy production.

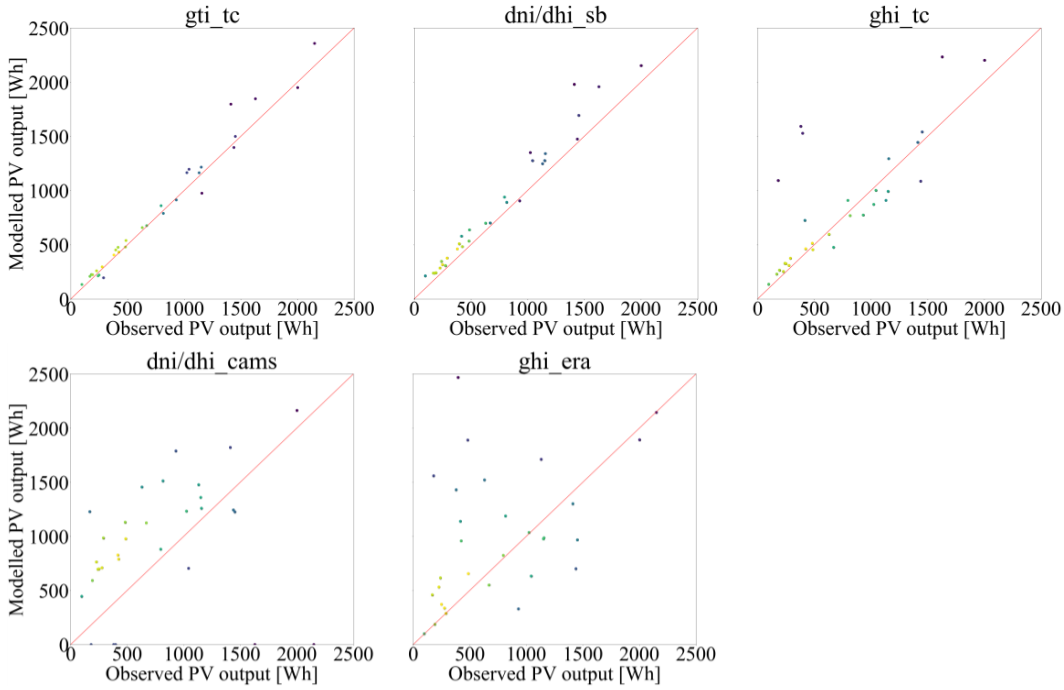

Fig. 7: Daily observed photovoltaic energy production and modelled photovoltaic energy production during October 2021, before the application of the data quality filter. The yellow color indicates a high datapoint density, while the blue color represents a low datapoint density.

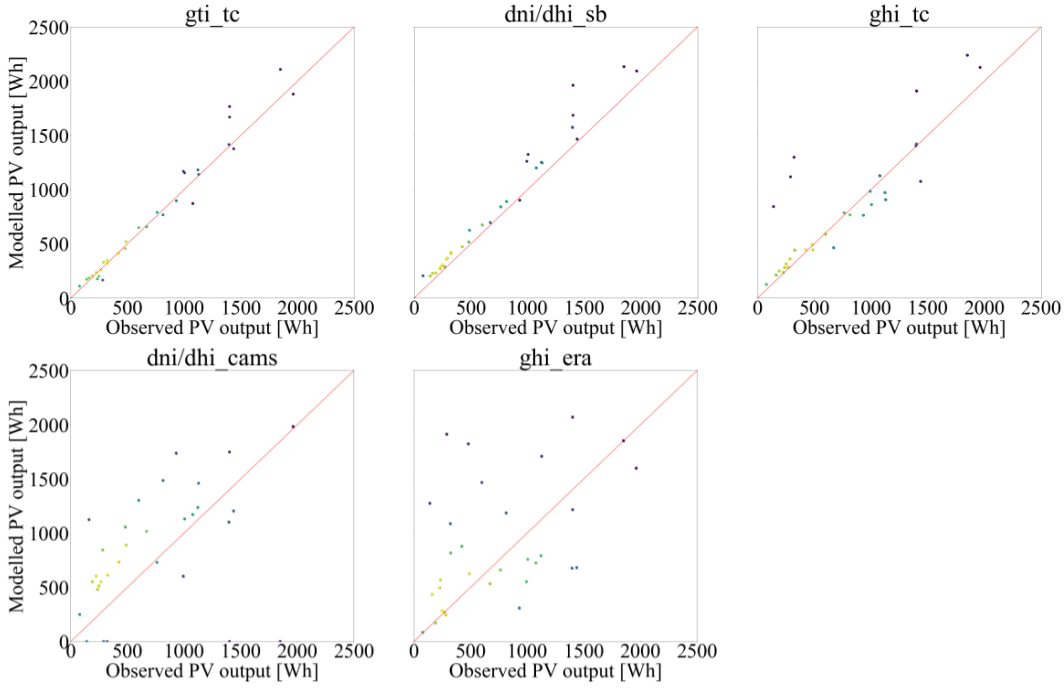

Fig. 8: Daily observed photovoltaic energy production and modelled photovoltaic energy production during October 2021, after the application of the data quality filter. The yellow color indicates a high datapoint density, while the blue color represents a low datapoint density.

The solar radiation datasets with POA amounts from the Test Cell Lab is the one with the lowest accuracy indicators (Tab. 3). In particular, the MBE of the gti_tc ranges from 40.77 Wh (before DQF) to 28.70 Wh (after DQF), while the RMSE is 107.58 Wh (before DQF) and 115.63 Wh (after DQF). Again, the worst performance

is observed for datasets derived from satellite observations and numerical analysis.

Tab. 3: Accuracy indicators calculated for the daily datasets exploited in this study.

	gti_tc	dni/dhi_sb	ghi_tc	dni/dhi_cams	ghi_era
MBE [Wh]	40.77	136.38	147.05	165.95	268.69
RMSE [Wh]	107.58	182.50	396.89	673.84	669.93
MBE (DQF) [Wh]	28.70	120.02	93.00	111.55	164.49
RMSE (DQF) [Wh]	115.63	166.29	306.37	577.11	592.72

Regarding the PV simulation over the whole month, the residues between the modelled and the monitored PV energy production values are presented (Table 4). Residues are expressed as a percentage, and they are defined as the difference between the model output and the observed value. The energy from the PV panel equals 23,954 Wh before the application of the DQF and 20,160 Wh after the DQF. The comparation of the residues confirm the gti_tc as the best dataset to estimate PV energy generation, while the ghi_tc turns out to be worse than datasets from satellite observations if DQF is not applied.

Tab. 4: Residues calculated between the observed and calculated monthly photovoltaic energy generation.

	gti_tc	dni/dhi_sb	ghi_tc	dni/dhi_cams	ghi_era
Before DQF [Wh]	5.01%	15.01%	16.18%	33.98%	26.36%
After DQF [Wh]	3.78%	14.08%	11.27%	28.52%	18.67%

3.2. Discussion

High-resolution datasets based on satellite imaging methods (i.e., CAMS) are found to be more accurate than one-hour datasets based on numerical weather prediction and assimilation methods (i.e., ERA5-Land global reanalysis) in Trondheim. A similar result was observed by Kenny and Fiedler (Kenny and Fiedler, 2022) in 30 locations in Germany. However, diffuse, and direct irradiance values which are measured by weather stations are generally preferable to those derived from satellite observations due to the lower error associated to the monitoring equipment, even if the two components are rarely measured (Manni et al., 2023). In fact, pyranometers measuring GHI are commonly used in solar monitoring campaign due to their lower investment costs if compared to the sun tracker equipment.

Based on the preliminary outcomes from this work, the length of the model chain determines the accuracy of the modelled PV energy generation more than the time resolution of the datasets. When variables measured by weather stations are considered, the one-hour POA dataset outperforms the one-minute dataset with monitored DNI and DHI values; it performs better than the GHI dataset having a time resolution of five minutes.

Finally, the following recommendations are carried out from this study:

- When available, solar radiation data from weather stations should be prioritized despite of their time resolution.
- DHI and DNI values from monitoring campaign or satellite imaging methods should be used instead of GHI datasets to reduce the length of the model chain.
- Measuring POA is also a valid option since it combines the short model chain to the low costs of the monitoring sensor (i.e., pyranometer).

3.3. Limitations of the study

In this section, the limitations of the study are outlined and commented. Firstly, the selected time interval is only one-month so the results are affected by the specific weather conditions and by the specific selected period of the year. In fact, datasets that perform badly in the overcast conditions in October 2021 (i.e., the analysis period)

might perform better during those months which show prevalently clear sky conditions (i.e., July, August). However, this study allows carrying out some preliminary considerations about the accuracy of the investigated model chains.

Secondly, October 2021 was mostly characterized by overcast sky conditions in Trondheim that affect the validity of the results. However, most of the numerical model and datasets are able to model PV energy generation during clear sky days, while simulating overcast sky conditions is more challenging.

Thirdly, the use of a single decomposition and transposition model can limit the reliability of the results. In fact, the use of a more effective combination of decomposition and transposition models could led to lower accuracy indicators for those datasets containing data about GHI or DNI and DHI. On the contrary the use of a different energy model for the simulation of the PV system would have had a less remarkable impact on the results since it is applied to all the datasets. Despite of that, the use of decomposition and transposition models and the longer model chain imply a low accuracy of the results.

4. Conclusive remarks

A comparative analysis of different solar radiation datasets and their capability of simulating PV is carried out. One-month solar radiation datasets from satellite observations, numerical reanalysis and weather stations are used as input parameters in the model chain combining the Engerer4 decomposition model and the Perez transposition model with the energy model described in sub-section 2.3. Outputs are compared against experimental data collected from the PV panel installed on the roof of the Test Cell Lab. The achievements from this study contribute to determine suitable irradiance dataset to be exploited in the model chain for the prediction of mono-facial PV energy generation at high latitudes as Trondheim.

The main findings are summarized in the following bullets:

- The POA data collected every hour in Test Cell Lab permit to estimate the hourly PV energy generation with the highest accuracy after the application of the data quality control filter (MBE is 2.65 Wh, RMSE is 39.78 Wh).
- Accuracy indicators calculated for the datasets based on observations are lower than the ones calculated for datasets based on satellite imaging or numerical reanalysis.
- Daily and monthly aggregation of the hourly datasets confirmed the POA data to better simulate the daily and monthly energy produced by the investigated PV panel.

Further insights into the model chain and solar radiation datasets are necessary. This includes:

- Assessing the capability of solar radiation datasets to estimate PV production over a wider time horizon such as one or more years instead of a single month.
- Performing a sensitivity analysis on different combinations of decomposition and transposition models to identify the most effective model chain at high latitude locations.
- Reiterate the comparative analysis for different PV panel technologies such as bi-facial PV systems which require a more accurate evaluation of the diffuse fraction.
- Validating the implemented model chain with experimental data from different high-latitude locations and different PV systems.

5. Acknowledgments

The authors acknowledge the financial support from the Norwegian Research Council (research project FRIPRO-FRINATEK no. 324243 HELIOS).

6. References

Bright, J.M., Engerer, N.A., 2019. Engerer2: Global re-parameterisation, update, and validation of an irradiance separation model at different temporal resolutions. J. Renew. Sustain. Energy 11, 33701.

https://doi.org/10.1063/1.5097014

Dubey, S., Sarvaiya, J.N., Seshadri, B., 2013. Temperature dependent photovoltaic (PV) efficiency and its effect on PV production in the world - A review, in: Energy Procedia. Elsevier, pp. 311–321. https://doi.org/10.1016/j.egypro.2013.05.072

Energy Facts Norway, 2021. Electricity Production [WWW Document]. URL https://energifaktanorge.no/en/norsk-energiforsyning/kraftproduksjon/ (accessed 3.27.22).

Formolli, M., Lobaccaro, G., Kanters, J., 2021. Solar energy in the Nordic built environment: challenges, opportunities and barriers. Energies 14. https://doi.org/10.3390/en14248410

Gueymard, C.A., 2017. Cloud and albedo enhancement impacts on solar irradiance using high-frequency measurements from thermopile and photodiode radiometers. Part 2: Performance of separation and transposition models for global tilted irradiance. Sol. Energy 153, 766–779. https://doi.org/10.1016/J.SOLENER.2017.04.068

Hay, J.E., 1993. Calculating solar radiation for inclined surfaces: Practical approaches. Renew. Energy 3, 373–380. https://doi.org/10.1016/0960-1481(93)90104-O

Holmgren, W.F., Hansen, C.W., Mikofski, M.A., 2018. PVlib Python: a Python package for modeling solar energy systems. J. Open Source Softw. 3, 884. https://doi.org/10.21105/joss.00884

International Energy Agency, 2021a. Renewables Information: Overview [WWW Document]. URL https://www.iea.org/reports/renewables-information-overview (accessed 8.2.22).

International Energy Agency, 2021b. Net Zero by 2050 [WWW Document]. URL https://www.iea.org/reports/net-zero-by-2050 (accessed 8.2.22).

International Renewable Energy Agency, 2022. World Energy Transition - Outlook 2022: 1.5°C Pathway. Abu Dhabi.

Kenny, D., Fiedler, S., 2022. Which gridded irradiance data is best for modelling photovoltaic power production in Germany? Sol. Energy 232, 444–458. https://doi.org/10.1016/J.SOLENER.2021.12.044

Loutzenhiser, P.G., Manz, H., Felsmann, C., Strachan, P.A., Frank, T., Maxwell, G.M., 2007. Empirical validation of models to compute solar irradiance on inclined surfaces for building energy simulation. Sol. Energy 81, 254–267. https://doi.org/10.1016/j.solener.2006.03.009

Manni, M., Nocente, A., Bellmann, M., Lobaccaro, G., 2023. Multi-Stage Validation of a Solar Irradiance Model Chain: An Application at High Latitudes. Sustainability 15. https://doi.org/10.3390/su15042938

Reindl, D.T., Beckman, W.A., Duffie, J.A., 1990. Diffuse fraction correlations. Sol. Energy 45, 1–7. https://doi.org/10.1016/0038-092X(90)90060-P

Yang, D., 2022. Estimating 1-min beam and diffuse irradiance from the global irradiance: A review and an extensive worldwide comparison of latest separation models at 126 stations. Renew. Sustain. Energy Rev. 159, 112195. https://doi.org/10.1016/J.RSER.2022.112195

Nomenclature

Acronyms

RES	Renewable Energy Sources
GHG	Greenhouse Gas
PV	Photovoltaic
NTNU	Norwegian University of Science and Technology
ECMWF	European Centre for Medium-Range Weather Forecasts

ERA5-Land	ECMWF 5th generation reanalysis for land application
CAMS	Copernicus Atmosphere Monitoring Service
DQF	Data Quality Filter

Variables

GHI	Global Horizontal Irradiance [Wh]
DHI	Direct Horizontal Irradiance [Wh]
DNI	Direct Normal Irradiance [Wh]
POA	Plane of Array Irradiance [Wh]
MBE	Mean Bias Error [Wh]
RMSE	Root Mean Square Error [Wh]
E	Energy [Wh]
f_{perf}	Temperature-dependent losses for semi-integrated panels and other configurations
P	Power [kW]
I_{ref}	Reference conditions for the investigated PV panel [kW/m^2]
N	Number of elements in the series
$\bar{x}_i$	i-th calculated values
x_i	i-th observations

Subscripts

el	Electricity
out	Output
sol	Solar
pv	Photovoltaic
pk	Peak